Optical polarization anisotropy of tensile strained InGaN/AlInN quantum wells for TM mode lasers

Po-Yuan Dang (鄧博元) and Yuh-Renn Wu (吳育任)[a)]
Department of Electrical Engineering, Institute of Photonics and Optoelectronics, National Taiwan University, Taipei, Taiwan 10617, Republic of China

(Received 26 August 2010; accepted 30 August 2010; published online 22 October 2010)

In this paper, we discuss the optical characteristics and polarization anisotropy of a tensile strained polar *c*-plane InGaN/AlInN quantum well. We found that if the quantum well is under the tensile strain, the $|Z\rangle$-like state will be lifted up so that the emitted light will be TM mode. In addition, with a particular aluminum composition of the AlInN alloy as the barrier for the tensile strained InGaN quantum well, it is possible to reduce quantum-confined Stark effect. The self-consistent Poisson and 6×6 $k\cdot p$ Schrödinger solver has been used for studying light emitting characteristics. Our results show that the tensile strained InGaN quantum well on AlInN barrier has much larger optical gain and lower threshold carrier density compared to the conventional InGaN/GaN system, and it has a potential to be TM light source for edge emitting laser diodes with the photonic crystal cavity made by nanorod arrays. © *2010 American Institute of Physics*. [doi:10.1063/1.3498805]

I. INTRODUCTION

Recently, wurtzite III-nitride optoelectronic devices such as InGaN/GaN light emitting diodes and laser diodes have been widely used in several applications. Many studies are focusing on the potential applications of nanostructures, such as photonic crystal structures, nanoholes, and nanorods. In the studies of photonic band gap (PBG) technology suggest that: in the case of dielectric rod array or nanocolumns, a large gap is opened for TM mode but not for TE mode.[1] Therefore, if we want to use this kind of structures for the laser application, it requires a TM mode light source. However, in the conventional *c*-plane InGaN/GaN quantum well systems, the compressive strain is always induced in the active layer, and the polarization property of light is restricted to TE mode and nonpolarized since the $|X\rangle \pm i|Y\rangle$ mixed states subbands are always on top of valence band.[2] Furthermore, there is a strong internal electric field caused by the spontaneous and piezoelectric polarization charge at the interfaces of the *c*-plane InGaN/GaN quantum well. This phenomenon leads to the quantum-confined Stark effect (QCSE), decreases the internal quantum efficiency, and leads the emission spectrum to have a redshift. There are studies[3–5] investigating the interface polarization charges, which use quaternary alloy materials to improve the performance. In addition, many studies[6–9] have focused on the nonpolar and semipolar planes. These results have shown that the light emission will be polarized, and the QCSE will be reduced. However, due to the higher cost for the *a*-plane and *m*-plane substrates, it would be better to use the *c*-plane substrate to reduce the cost.

As we know, the band gap and lattice constant of the ternary $Al_xIn_{(1-x)}N$ cover an extremely large range, opening up some significant applications. In this work, we introduced the *c*-plane InGaN/AlInN quantum well structure instead of the conventional InGaN/GaN quantum well in order to obtain the tensile strain in the quantum well layer. In previous studies[10–12] and our calculation, it has shown that for nitride based materials, the $|Z\rangle$-like state raises up when the film is under the tensile lateral strain as shown in Fig. 1(a). The light emission will mainly be TM mode (*z*-polarized). To have a tensile strain in the quantum well, we can put the InGaN layer on top of certain AlInN barrier. As shown in Fig. 1(b), if we can grow the AlInN barrier on the GaN nanorods structures, the strain of AlInN barrier will be relaxed[13] and the InGaN quantum well will have a tensile strain. As we mentioned, nanorods structures have a large PBG for the TM mode. And the emitted light can be easily coupling into the photonic crystal structure. In addition, we also look for some particular alloy composition of the quantum well and the barrier with the tensile strain, which can also achieve polarization-match to eliminate the internal field and reduce the QCSE.

II. FORMALISM

To obtain the band structure, eigen levels, wave functions, and Fermi levels, we applied the self-consistent Pois-

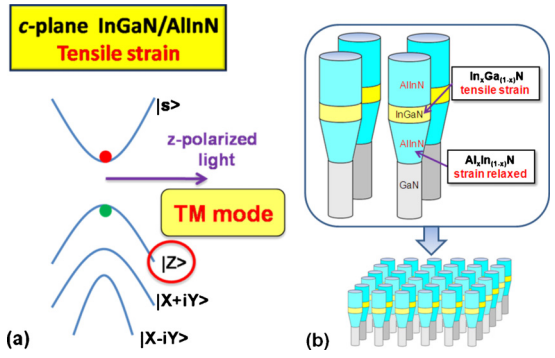

FIG. 1. (Color online) (a) The schematic band structure diagram of the *c*-plane InGaN/AlInN quantum well under the tensile strain. (b) The schematic of the nanorod structure.

[a)]Electronic mail: yrwu@cc.ee.ntu.edu.tw.

son and 6×6 $k\cdot p$ Schrödinger solver to solve iteratively until convergence. The $k\cdot p$ method[14] is used for calculating the valence band and the effective mass approximation method is used for calculating the conduction band. We use Eq. (1) to acquire the polarization-dependent optical matrix element,

$$x-polarized:|\langle S|p_x|X\rangle|^2(|\langle\psi_l^e|\psi_{m1}^h\rangle\uparrow+\langle\psi_l^e|\psi_{m5}^h\rangle\uparrow|^2 + |\langle\psi_l^e|\psi_{m2}^h\rangle\downarrow+\langle\psi_l^e|\psi_{m6}^h\rangle\downarrow|^2)/4,$$

$$y-polarized:|\langle S|p_y|Y\rangle|^2(|\langle\psi_l^e|\psi_{m1}^h\rangle\uparrow-\langle\psi_l^e|\psi_{m5}^h\rangle\uparrow|^2 + |\langle\psi_l^e|\psi_{m2}^h\rangle\downarrow-\langle\psi_l^e|\psi_{m6}^h\rangle\downarrow|^2)/4,$$

$$z-polarized:|\langle S|p_z|Z\rangle|^2(|\langle\psi_l^e|\psi_{m3}^h\rangle\uparrow+\langle\psi_l^e|\psi_{m4}^h\rangle\downarrow|^2)/2. \quad (1)$$

The bases of the valence band wave functions ψ_1^h-ψ_6^h are $1/\sqrt{2}|X+iY,\uparrow\rangle$, $1/\sqrt{2}|X+iY,\downarrow\rangle$, $|Z,\uparrow\rangle$, $|Z,\downarrow\rangle$, $1/\sqrt{2}|X-iY,\uparrow\rangle$, and $1/\sqrt{2}|X-iY,\downarrow\rangle$, respectively. The polarization of the emission light is strongly affected by these bases. Finally, we calculate the spontaneous emission rate, the optical gain, and threshold carrier density.[15] The optical gain is obtained by

$$g(\hbar\omega)=\frac{\pi e^2\hbar}{n_r c m_0^2\varepsilon_0\hbar\omega W}\sum_{i,j}\int\frac{2}{(2\pi)^2}d^2\vec{k} \times|\hat{a}\cdot\vec{p}_{i,j}|^2\frac{1}{\sigma\sqrt{2\pi}}\exp\left[\frac{-(E_{i,j}-\hbar\omega)^2}{2\sigma^2}\right] \times[f^e(E_i^e)-(1-f^h(E_j^h))]\ (\mathrm{cm}^{-1}), \quad (2)$$

where f^e and f^h are Fermi–Dirac function, n_r is the refractive index, W is the quantum well width, $E_{i,j}$ is the effective bandgap from the state i to j, σ is the inhomogeneous broadening factor, and $|\hat{a}\cdot\vec{p}_{i,j}|^2$ is the momentum matrix element between the electronic state i and the hole state j. In order to analyze the polarization, we define the polarization ratio as

$$\rho=\frac{I_z-I_{(x+y)}}{I_z+I_{(x+y)}}, \quad (3)$$

where I_x, I_y, and I_z are the emission intensity of x, y, and z-polarized light, respectively. The details of the self-consistent numerical model and $k\cdot p$ formalism are presented in previous studies.[8,9]

III. RESULT

To reduce the QCSE, we need to find the condition for the polarization match at InGaN/AlInN interface, i.e., $\Delta P_z=(P_{ez}+P_{sp})_{\mathrm{InGaN}}-(P_{sp})_{\mathrm{AlInN}}=0$. P_{ez} is the piezoelectric polarization induced by the tensile strain. P_{sp} is the spontaneous polarization of the InGaN quantum well and AlInN barrier. For the case of $In_{0.2}Ga_{0.8}N/Al_xIn_{(1-x)}N$, ΔP_z is almost zero when Al composition is ~54%. Under this condition, the QCSE is minimized. Compared with the compressive strain, the main reason for this phenomenon is due to the tensile strain effect induced in the InGaN quantum well where the induced piezoelectric polarization is in different direction to cancel the spontaneous polarization. When the indium compositions of the quantum well are 10%, 30%, and 40%, the Al compositions for the polarization matching are ~61%, ~47%, and ~41%, respectively. Table I shows the estimated lateral tensile strain of InGaN layers on these different AlInN barriers, which are still in a reasonable strain range.

TABLE I. The calculated lateral strain of InGaN layers in different AlInN barriers.

Configuration	$\varepsilon_{\parallel}$ in InGaN layer (%)
$In_{0.1}Ga_{0.9}N/Al_{0.61}In_{0.39}N$	1.69
$In_{0.2}Ga_{0.8}N/Al_{0.54}In_{0.46}N$	1.51
$In_{0.3}Ga_{0.7}N/Al_{0.47}In_{0.53}N$	1.32
$In_{0.4}Ga_{0.6}N/Al_{0.41}In_{0.59}N$	1.13

Figure 2(a) shows the optical matrix element of $|X\rangle$, $|Y\rangle$, and $|Z\rangle$ components in the first subband versus k_x with zero internal field in the case of $In_{0.2}Ga_{0.8}N$ quantum well. We can find the topmost subband state is dominated by $|Z\rangle$ state, and there is almost no mixing of other states. The z-polarized light is remarkably dominated in the entire k-space. For carrier with higher energy, the wave is less confined in the quantum well and the electron-hole overlapping decreases. Therefore, we can find that all components decreases as k vector increases. Figure 2(b) shows that the ratio of z-component increases as k_x increases. The trend along k_y direction is the same because of the isotropic strain in the in-plane direction. Therefore, a strong z-polarized light emission will be measured at the in-plane direction.

To compare the emission strength, we show the comparison of the spontaneous emission spectra for both the $In_{0.2}Ga_{0.8}N/Al_{0.54}In_{0.46}N$ quantum well with zero internal field and the conventional $In_{0.2}Ga_{0.8}N/GaN$ quantum well in Fig. 3. In the conventional quantum well, light emission is mixed with x-polarized and y-polarized and is nonpolarized. In the case of AlInN barrier, light emission is z-polarized dominated, the polarization ratio is 87% at injection carrier density equal to 2×10^{19} cm^{-3}. Also, we find that the emission peak has a stronger intensity and does not have a large redshift compared to the conventional case. In the case of AlInN barrier, the QCSE effect has noticeably eliminated.

Figures 4(a) and 4(b) show the comparison of the optical gain for the $In_{0.2}Ga_{0.8}N/Al_{0.54}In_{0.46}N$ quantum well and the

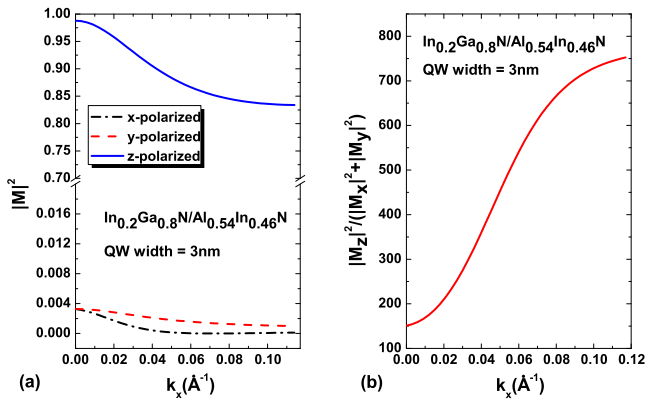

FIG. 2. (Color online) (a) The optical matrix element of $|X\rangle$, $|Y\rangle$, and $|Z\rangle$ components in the first subband vs k_x. (b) The ratio $|M_z|^2/(|M_x|^2+|M_y|^2)$ in the first subband vs k_x.

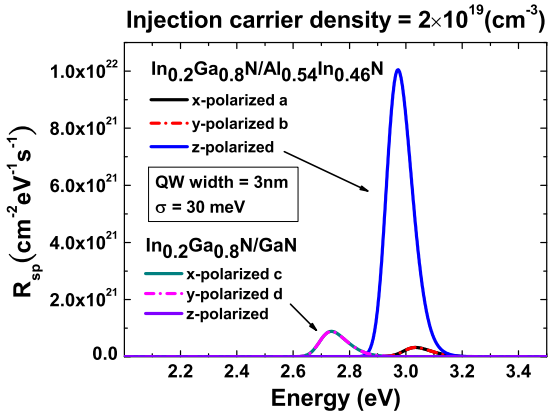

FIG. 3. (Color online) The polarization-dependent spontaneous emission spectra of the $In_{0.2}Ga_{0.8}N/Al_{0.54}In_{0.46}N$ quantum well with zero internal field and the conventional $In_{0.2}Ga_{0.8}N/GaN$ quantum well. Note that the curves for a and b are overlapped and the curves for c and d are also overlapped.

conventional $In_{0.2}Ga_{0.8}N/GaN$ quantum well with different injection carrier densities, respectively. We can find that the optical gain of the AlInN barrier case is much larger than the conventional case. In the conventional case, the optical gain of *x*-polarized is equal to *y*-polarized due to the in-plane isotropy, and the optical gain of the AlInN barrier case is *z*-polarized light dominated. In addition, attributing to the higher differential gain, the optical gain of the AlInN barrier

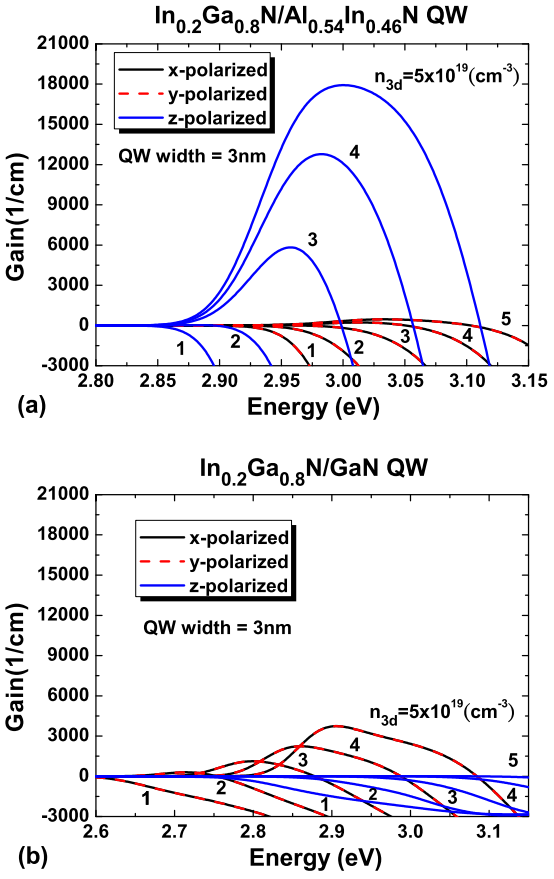

FIG. 4. (Color online) (a) and (b) are the optical gain spectra of the $In_{0.2}Ga_{0.8}N/Al_{0.54}In_{0.46}N$ quantum well with zero internal field and the conventional $In_{0.2}Ga_{0.8}N/GaN$ quantum well for carrier density n_{3d} from 1×10^{19} cm^{-3} up to 5×10^{19} cm^{-3}, respectively.

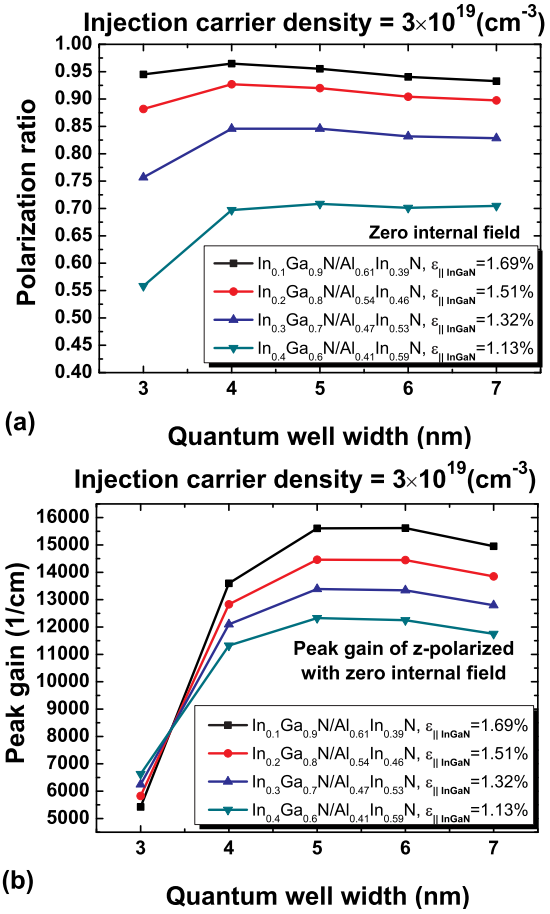

FIG. 5. (Color online) (a) The polarization ratio of light as a function of quantum well width with different indium compositions of quantum well. (b) The peak gain of the *z*-polarized light as a function of quantum well width with different indium compositions of quantum well. Note that all cases are designed with zero internal field, and the isotropic in-plane strain for indium compositions of the InGaN QW from 10% to 40% are 1.69%, 1.51%, 1.32%, and 1.13%, respectively.

case increases sooner than the conventional case. The peak gain for the AlInN barrier case increases significantly due to its improved transition matrix element. At injection carrier density equal to 3×10^{19} cm^{-3}, the peak gain for the AlInN barrier case is 5.2 times improvement compared to the conventional case. In order to evaluate the feasibility of the tensile strained InGaN/AlInN quantum well for diode lasers application, we employed a laser structure with a quantum well as active region.[16,17] We assumed the optical confinement factor Γ is 1%, internal loss is 17.7 cm^{-1}, and mirror loss is 25 cm^{-1}. The threshold gain required for lasing is ~4270 cm^{-1}. The threshold carrier density of the AlInN barrier case is 2.8×10^{19} cm^{-3}, which corresponds to 47% reduction compared to that ($n_{th}=5.3\times10^{19}$ cm^{-3}) of the conventional case. The reduction in the threshold carrier density is important. It will lead to the reduction in the nonradiative component of the threshold current density.

In the quantum well system, we need to consider not only the strain effect but also the quantum confinement effect. Figures 5(a) and 5(b) show the change of the polarization ratio and the peak gain of the *z*-polarized light as a function of quantum well width with different indium compositions of the quantum well, respectively. Note that all

cases are designed to have zero internal field. As shown in Fig. 5, the polarization ratio and peak gain are larger in lower indium composition of the quantum well. In order to make the zero internal field condition, the quantum wells with different indium compositions are with different AlInN alloy compositions. Therefore, in these cases, the 10% indium composition has the largest tensile strain, which leads to a larger polarization ratio. For the quantum well width from 3 to 5 nm, the polarization ratio and peak gain increase due to changes of *E-k* dispersion curve and weaker quantum confinement effect. In the valence band, the energy minimum of hole in the first subband of the valence band is shifted slightly from the Γ point in the small quantum well width, which reduce the radiative recombination rate. For the larger quantum well width, energy minimum center shifts back to Γ point and the peak gain is saturated as the quantum well width increases.

IV. CONCLUSION

In conclusion, we have studied the tensile strain effect and the light emission polarization properties in InGaN quantum well with the AlInN barrier layer. Our results suggest that using the AlInN to be the barrier material with optimized alloy composition in the tensile strained InGaN quantum wells will not only have the polarized light emission but also eliminate the QCSE to enhance emission performance. In our calculation, both the spontaneous emission spectra and the optical gain of the tensile strained InGaN/AlInN quantum well exhibit enhancement in comparison to the conventional InGaN/GaN quantum well. The improvement of the optical gain in the tensile strained InGaN/AlInN quantum well with zero internal field results in the reduction in threshold carrier density. The tensile strain is helpful to emit TM mode for the output light in the in-plane direction, which would be applicable in nanorods photonic crystal structures for laser applications.

[1] R. D. Meade, A. M. Rappe, K. D. Brommer, and J. D. Joannopoulos, J. Opt. Soc. Am. B **10**, 328 (1993).
[2] S. H. Park, D. Ahn, and S. L. Chuang, IEEE J. Quantum Electron. **43**, 1175 (2007).
[3] M. F. Schubert, J. Xu, J. K. Kim, E. F. Schubert, M. H. Kim, S. Yoon, S. M. Lee, C. Sone, T. Sakong, and Y. Park, Appl. Phys. Lett. **93**, 041102 (2008).
[4] M. H. Kim, W. Lee, D. Zhu, M. F. Schubert, J. K. Kim, E. F. Schubert, and Y. Park, IEEE J. Sel. Top. Quantum Electron. **15**, 1122 (2009).
[5] S. H. Park, D. Ahn, and J. W. Kim, Appl. Phys. Lett. **92**, 171115 (2008).
[6] A. E. Romanov, T. J. Baker, S. Nakamura, J. S. Speck, and E. J. U. Grp, J. Appl. Phys. **100**, 023522 (2006).
[7] A. A. Yamaguchi, Appl. Phys. Lett. **94**, 201104 (2009).
[8] H. H. Huang and Y. R. Wu, J. Appl. Phys. **106**, 023106 (2009).
[9] H. H. Huang and Y. R. Wu, J. Appl. Phys. **107**, 053112 (2010).
[10] M. Nido, Jpn. J. Appl. Phys., Part 2 **34**, L1513 (1995).
[11] S. Chichibu, T. Azuhata, T. Sota, H. Amano, and I. Akasaki, Appl. Phys. Lett. **70**, 2085 (1997).
[12] D. Fu, R. Zhang, B. Wang, Z. Zhang, B. Liu, Z. Xie, X. Xiu, H. Lu, Y. Zheng, and G. Edwards, J. Appl. Phys. **106**, 023714 (2009).
[13] H. S. Chen, D. M. Yeh, Y. C. Lu, C. Y. Chen, C. F. Huang, T. Y. Tang, C. C. Yang, C. S. Wu, and C. D. Chen, Nanotechnology **17**, 1454 (2006).
[14] S. Ghosh, P. Waltereit, O. Brandt, H. T. Grahn, and K. H. Ploog, Phys. Rev. B **65**, 075202 (2002).
[15] J. Singh, *Electronic and Optielectronic Properties of Semiconductor Structure* (Cambride, United Kingdon, 2007).
[16] H. P. Zhao, R. A. Arif, Y. K. Ee, and N. Tansu, IEEE J. Quantum Electron. **45**, 66 (2009).
[17] H. Y. Ryu, K. H. Ha, S. N. Lee, T. Jang, J. K. Son, H. S. Paek, Y. J. Sung, H. K. Kim, K. S. Kim, O. H. Nam, Y. J. Park, and J. I. Shim, IEEE Photonics Technol. Lett. **19**, 1717 (2007).